To the problem of cross-bridge tension in steady muscle shortening and lengthening

.

By Valery B. Kokshenev

.

Submitted to the Journal of Biomechanics 14 April 2009, BM-D_09-00317

.

Departamento de Física, Universidade Federal de Minas Gerais, Instituto de Ciências Exatas, Caixa Postal 702, CEP 30123-970, Belo Horizonte, Brazil, valery@fisica.ufmg.br

.

Abstract. Despite the great success of the Huxley sliding filament model proposed half a century ago for actin-myosin linkages (cross-bridges), it fails to explain the force-velocity behavior of stretching skeletal muscles. Huxley's two-state kinetic equation for cross-bridge proportions is therefore reconsidered and a new solution to the problem of steady muscle eccentric and concentric contractions is reported. Instead of numerical modeling the contractive-force data by appropriate choice of the seemingly arbitrary heterogeneity of attachment and detachment rates of myosin heads to actin filament cites, Huxley's idea on mechanical equilibrium is probed into thermodynamic equilibrium in the whole overlapped actin-myosin zone. When the second law of statistical thermodynamics is applied to cross-bridge proportions, the weakly bound states appear to be correlated to the strongly bound states via structural and kinetic intrinsic muscle characteristics. A consequent substantial reduction of the number of free parameters in cross-bridge proportions is also due to the overall self-consistency (normalization) of attachment-detachment stochastic events. The explicit force-velocity curve is found to be generic when applied to the reduced tension in a single cross bridge, sarcomere, fiber, or muscle as a whole during its active shortening or lengthening. This universal curve fits the empirical tension-velocity data on frog muscle shortening using only one adjustable parameter, while the Huxley model employed four parameters. The established normally distributed cross-bridges, detaching slowly near equilibrated states in steady lengthening muscle and quickly in shortening muscle, are in qualitative agreement with recent data on the force enhancement following muscle stretching.

.

1. Introduction

The early studies of muscle fibers under the light microscope revealed cross-striations running normal to the fiber axis. It was observed that during either concentric or eccentric contractions, the length changes occurred via an increase or decrease in the extent of the I-band with the A-band remaining unchanged. Two groups laid the foundations for the cross-bridge (CB) theory when they simultaneously suggested that muscle contractions occur due to the relative sliding of the thick myosin filaments past the thin actin filaments, mediated by the ATP-dependent actin-myosin linkages (H. E. Huxley and Hanson, 1954) working as independent force generators (A. F. Huxley and Niedergerke, 1954).

A. F. Huxley (1957) evaluated muscle tension caused by shortening, in fact, based on the idea of the existence of *mechanical* equilibrium of myosin heads at the regular sites of actin filaments. His famous two-state (bound-unbound) sliding filament model was determined on the basis of the simplest standard kinetic equation controlled by the velocity-independent rates of attachment and detachment of myosin heads. In spite of the great success in illuminating the force generation and power liberation during muscle shortening, the Huxley approach generally failed to explain the ascending branch of the phenomenologically established tension-velocity equation (see e.g. Harry et al., 1990 and references therein).

Exploring the fact that the sliding filament model leaves a free choice of the attachment and detachment rate functions, many researchers successfully simulated a range of muscle properties in lengthening by fitting the empirical data by linear functions and constants suggested by Huxley (1957) for the CB proportions or by bilinear and exponential functions. Likewise, considerable efforts have been made to modify the rate functions (Zahalak, 1981; Harry et al., 1990; Ma and Zahalak, 1991; Cole et al., 1996) or to find an exact *numerical* solution to Huxley's model (Wu et al., 1997). Very recently, controversies surrounding Huxley's approach were brought forth by Mehta and Herzog (2008) in their careful studies of force exposed by a single CB during lengthening.

The theoretical problem of self-consistency in the two-state sliding filament models was thoughtfully discussed by Hill and co-workers (Hill et al., 1975). Considering the conditions of CB *thermodynamic* equilibrium besides the minimum of mechanical energy (Huxley, 1957), they demonstrated that the original Huxley model has a low efficiency in comparison to its modified versions. Moreover, it was noted by Eisenberg et al. (1980) that "there is no in vitro evidence for ... the basic (Huxley's) assumption that the cross-bridge detaches slowly".

The lacking data were provided by Mehta and Herzog (2008).

In this study, I develop a statistical approach to the filament sliding mechanism and show that only linear functions for the attachment-detachment rates are compatible with the concept of thermodynamic equilibrium. A new analytical solution to Huxley's two-state kinetic equation is proposed and verified using the available from the literature data on tension in steady muscle lengthening and shortening.

.

2. Methods

2.1. Model by Huxley (1957) revisited

At a fixed muscle *contraction velocity* V, the number of bound CB states N_V combining myosin filament with actin filament of the total number of sites N_{0A} obeys the common "balance" kinetic equation

$$\frac{d}{dt}N_V(x,t) = \frac{\partial N_V}{\partial t} + \frac{\partial N_V}{\partial x}\cdot\frac{dx}{dt} = \ f(x)(N_{0A} - N_V) - g(x)N_V. \tag{1}$$

Here f and g are *attachment* and *detachment rates* of the corresponding unbound and bound states located in time t at a distance x estimated from the nearest site $x = 0$. The steady process determined by late times $t \gg f^{-1},\ g^{-1}$ providing $\partial N_V(x,\infty)/\partial t = 0$ in Eq. (1), reduces Eq. (1) to

$$-\frac{V}{2}\frac{d}{dx}n_V(x) = \ f(x)(1 - n_V) - g(x)n_V, \tag{2}$$

i.e., to Huxley's Eq. (4) where the *proportion* $n_V(x) = N_V(x,\infty)/N_{0A}$ of CBs during *steady shortening*. According to Huxley, the force output $F(x) = kx$ is produced when x decreases at a positive velocity of sliding of the actin filament V_A and a negative velocity of myosin filament V_M, i.e., $V_A = -V_M = -dx/dt > 0$. The contraction velocity per one-half sarcomere $V/2$ determines the contraction *velocity* V of the muscle as a whole, when modeled by $V = V_A - V_M = 2V_A$. As can be derived from Huxley's Eq. (6) with the preservation in part its notations, the overall generated force

$$F_V^{(total)} = \lim_{L\to\infty}\frac{sN_{0M}}{L}\int_{-L}^{+L}F(x)n_V(x)\frac{dx}{2l_A}, \tag{3}$$

was evaluated via the force $F(x)$ per one *myosin site*, as one actin site is carried past it. Here s is the sarcomere length, l_A is the *trial* distance between the nearest sites in the actin filament *evaluated* in Huxley's Eq. (15), and N_{0M} is the number of sites in the thick filament in the overlapping zone of length L.

The solution to Eq. (2) for the shortening regime (hereafter distinguished by index 1) was found as a combination of the *localized* (short-domain) and *delocalized* (large-domain) spatially correlated (bound) states. The corresponding proportions reproduced exactly from Huxley's Eqs. (7) and (8) are

$$n_V^{(loc)}(x) = n_{01}\left(1 - \exp\left[\frac{V_1}{V}\left(\frac{x^2}{h^2} - 1\right)\right]\right),\ 0 \le x \le h \tag{4}$$

and

$$n_V^{(deloc)}(x) = n_{01}\left[1 - \exp\left(-\frac{V_1}{V}\right)\right]\exp\left(2x\frac{g_1'}{V}\right),\ -\infty < x \le 0, \tag{5}$$

though parameterized here by

$$n_{01} = \frac{f_1}{f_1 + g_1} \text{ and } V_1 = h(f_1 + g_1). \tag{6}$$

In turn, this description of the two CB states follows from the rates *postulated* by linear functions, namely

$$f(x) = f_1\frac{x}{h} \text{ and } g(x) = g_1\frac{x}{h}, \text{ for } 0 \le x \le h, \tag{7}$$

and two constants $f'(x) = 0$, $g'(x) = g_1'$, for $-\infty < x < 0$. The muscle concentric steady tension P_V reduced to the model isometric tension P_0 found on the basis of Eqs. (3)-(7), namely

$$\frac{P_V^{(short)}}{P_0} = 1 - \frac{V}{V_1}\left[1 - \exp\left(-\frac{V_1}{V}\right)\right]\left(1 + \frac{VV_1}{2h^2g_1'^2}\right), \text{ for } V > 0, \tag{8}$$

was fitted by the widely cited four model parameters: $f_1 = 43.3\ s^{-1}$ and $g_1 = 10.0\ s^{-1}$, indicating slow detachment of the localized CBs, and $f_1' = 0$ with $g_1' = 209\ s^{-1}$, for delocalized states. In addition, two more adjustable parameters $h \approx 15\ nm$ and $V_1 = V_{\max}^{(\exp)}/4$, where $V_{\max}^{(\exp)}$ is the empirical maximum shortening velocity, were indirectly employed when tested by Hill's empirical equation (see Chapter IV in Huxley, 1957). It is noteworthy that the nearest-site distance in the actin filament treated as a free parameter was estimated as $l \approx h$, i.e. close to the known nearest-molecular distance in the myosin filament $l_M = 14.5$ nm (Craig and Woodhead, 2006). However, the ratio $P_{-\infty}/P_0 = (f_1+g_1)/g_1 = 5.33$ reported by Huxley (1957) for the muscle lengthening regime, contrasts to the observed ratios falling between 1.8 and 2.0 (e.g. Harry et al., 1990).

.

2.2. A new solution to Huxley's steady equation

Beyond any specific suggestions, the formal solution to the steady-state Eq. (2)

$$n_V(x) = n_0(x) + \Delta n_V(x) = n_0 + (1 - n_0) c_V \exp\left(-\frac{1}{\dot{x}} \int_0^x [f(x') + g(x')] dx' \right), \; \dot{x} \equiv \frac{dx}{dt} = \mp \frac{V}{2}, \tag{9}$$

is valid for any contraction shortening velocity V $(= -2\dot{x} > 0)$ and lengthening velocity V $(= 2\dot{x} < 0)$, leaving an arbitrary choice of the rate functions $f(x)$ and $g(x)$. A differential equation of the first order possesses as common only one free constant, denoted by c_V, whereas

$$n_0(x) = \frac{f(x)}{f(x) + g(x)} \tag{10}$$

straightforwardly following from Eq. (2) taken at $V = 0$, describes maximal CB proportions limited by intrinsic rates. In the Huxley model, the constant $c_V = -n_{01}(1 - n_{01})^{-1} \exp(-V_1/V)$ in Eq. (9) results from his *boundary condition* $n_V(h) = 0$ providing the *non-Gaussian* proportion (4) for CB localized states during muscle shortening.

Besides the boundary conditions considered below, let us employ the property of periodicity in the overlapping part of the actin filament of length Nd having N *occupied cells*. Since the Huxley proportion $n_V(x)$ in Eq. (9) plays the role of the late-time *probability* of finding one of the two myosin heads attached at a position x between two nearest equivalent sites (see also Hill et al. 1975, p. 346), the total force output in a *finite* overlapped zone is

$$F_V^{(zone)} = N F_V = \int_{-Nd}^{+Nd} F(x') n_V(x') \frac{dx'}{2d} = N \int_{-d}^{d} F(x) n_V(x) \frac{dx}{2d}, \text{ where } x' = xN. \tag{11}$$

Here $F(x)$ is the active force *per one actin site*, substituting that per one myosin cite in Eq. (3). Such a consideration suggests the statistical equivalence of all the occupied cells in the actin filament treated as a one-dimensional crystal of lattice constant d $(= 36\ nm$, e.g. Hill et al., 1975). In order to be consistent with Eqs. (11) and (3), the normalization conditions for the CB distributions (proportions)

$$\int_{-d}^{+d} n_V(x) \frac{dx}{2d} = \int_0^d n_V(x) \frac{dx}{d} = \int_{-d}^{0} n_V(x) \frac{dx}{d} = 1 \tag{12}$$

must be taken into consideration.

Furthermore, extending Huxley's idea on the minimum of mechanical energy at $x = 0$ over the minimum of Gibbs energy (Eisenberg et al., 1980), the CB state with $F(0) = 0$ is treated as the locally equilibrated state, having *maximum configurational entropy* at $x = 0$. As the consequence of one of the most general principle (second law) of statistical thermodynamics,

the distribution of bound states $n_V(x)$ given in Eq. (9) must have Gaussian form centered at $x = 0$ (see e.g. Chapter 12 in Landau and Lifshitz, 1989). One can see from Eq. (9), that the thermodynamical principle ensured by the *sign requirement* $\dot{x}x > 0$ can be satisfied solely by the linear parameterization of the rate functions, namely

$$f(x) = f_m \frac{x}{x_m},\ g(x) = g_m \frac{x}{x_m},$$
$$\text{for } x_m = x_+ \geq x \geq 0 \text{ or } x_m = -x_- \leq x \leq 0, \tag{13}$$

Consequently, the normalization constant

$$c_V = \frac{d}{|x_m|} \frac{2}{\sqrt{\pi v}} \operatorname{erf}\left(\frac{1}{\sqrt{v}}\right)^{-1},\ v = \frac{V}{V_m} = \frac{2\dot{x}}{(f_m + g_m)x_m} > 0, \tag{14}$$

readily follows from the normalization conditions (12), where the standard *error function* $\operatorname{erf}(y) = (2/\sqrt{\pi}) \int_0^y \exp(-t^2)dt$, lying between 0 [$= \operatorname{erf}(0)$] and 1 [$= \operatorname{erf}(\infty)$], is employed.

.

3. Results

3.1. CB proportions in steady muscle shortening and lengthening

As seen in Eq. (9), a given CB is characterized by the equilibrated velocity-independent *ground* state and the *excited* non-equilibrated state described, respectively, by uniform proportion $n_0 = f_m/(f_m + g_m)$ and non-uniform, heterogenous stochastic proportion $\Delta n_V(x)$, having the meaning of probabilities normalized in Eq. (12). The requirement of signs ($\dot{x}x > 0$), while in particular ensuring the self-consistency with the ground state (when $x \to 0$, $\Delta n_V(x) \to 0$), also constrains possible domains for both CB states, as shown in Eq. (13). Indeed, both kinds of domains ($0 \leq x \leq x_0$ and $-x_0 \leq x \leq 0$, otherwise $n_0(x) = 0$) are generally possible for the ground state, whereas only the negative domain, $-x_- \leq x \leq 0$, satisfies the requirement of self-consistency of the solution given in Eq. (9). In this way, the CB boundary conditions are not postulated as in Eqs. (4)-(7), but result from the minimum of Gibbs energy, also giving rise to the CB *mechanical constraints*, consistent with the simultaneous observations of directions of both the force output and contraction velocity, as illustrated in Fig. 1.

.

Place Fig. 1

.

The analysis in Fig. 1 specifies domains of the *short-domain* CB states which, being incorporated in the trial Eq. (9) with the help of Eq. (14), yield

$$n_V(x) = n_0\Theta_0(x) + (1 - n_0\frac{x_0}{d})\frac{d}{x_-}\frac{2}{\sqrt{\pi v}}\frac{\exp\left(-\frac{x^2}{vx_m^2}\right)}{\mathrm{erf}\left(\frac{1}{\sqrt{v}}\right)}\Theta_V(x). \tag{15}$$

Here, the auxiliary functions $\Theta_0(x) = \Theta(\pm x) - \Theta(x \mp x_0)$ and $\Theta_V(x) \equiv \Theta(-x) - \Theta(x + x_-)$ are introduced by the standard Heaviside (step) function $\Theta(y)$, which is one for $y \geq 0$ and zero for $y < 0$.

.

3.2. Muscle tension in steady shortening and lengthening

The mean force output F_V generated by a single cell of the actin filament is evaluated using Eqs. (11) and (15), namely

$$F_V = F_0 + \Delta F_V = k\int_{-d}^{+d} x n_V(x)\frac{dx}{2d} = F_0 - k\frac{x_-}{2}(1 - n_0\frac{x_0}{d})\Phi(v),\ F_0 = \pm\frac{kx_0^2}{2d}n_0, \tag{16}$$

via the CB *stiffness* $k = F(x)/x$ (Huxley, 1957; Huxley and Simmons, 1971), shown to be a velocity-independent intrinsic muscle quantity (e.g. Lombardi and Piazzesi, 1990), where

$$\Phi(v) = 2\sqrt{\frac{v}{\pi}}\frac{1 - \exp(-\frac{1}{v})}{\mathrm{erf}(\frac{1}{\sqrt{v}})};\ \text{with } \Phi(0) = 0,\ \Phi(1) = 0.846,\ \text{and } \Phi(\infty) = 1. \tag{17}$$

The upper and lower signs in the velocity-independent limiting steady force F_0 (16) correspond to shortening and lengthening (see Fig. 1). In this way, Huxley's Eq. (8) is transformed into a unique equation

$$\frac{P_V}{P_0} = \frac{F_V}{F_0} = 1 \mp \sigma_m\Phi\left(v\right),\ \text{with } \sigma_m = \frac{(d - n_0x_0)x_-}{n_0x_0^2}, \tag{18}$$

for the reduced CB tension and force output in both concentric and eccentric muscle contractions conducted at positive and negative steady velocities $V = vV_m$ (14), respectively.

The *one-parameter* fitting analysis of the proposed theory is conducted on the basis of Eq. (18) and the available experimental data. In Fig. 2, the muscle shortening is described by

$$\frac{P_V^{(short)}}{P_{01}} = 1 - \frac{\Phi\left(\frac{\lambda V}{V_{\max}}\right)}{\Phi(\lambda)},\ 0 \leq V \leq V_{\max},$$
$$V_{\max} = \lambda V_{m1},\ V_{m1} = x_{m1}(f_{m1} + g_{m1}), \tag{19}$$

where λ is an adjustable parameter.

.

Place Fig. 2

.

.

Place Fig. 3

.

The steady muscle lengthening is fitted in Fig. 3 by

$$\frac{F_V^{(stret)}}{F_{02}} = 1 + \Phi\left(\frac{V}{V_{m2}}\right), \ -\infty < V \leq 0,$$
$$V_{m2} = -x_{m2}(f_{m2} + g_{m2}) < 0. \tag{20}$$

using the characteristic velocity V_{m2} as a free parameter. Other parameters describing two distinct regimes are specified as $x_- = x_{m1}$, $f_m = f_{m1}$, $g_m = g_{m1}$, for shortening, and $x_- = x_{m2}$, $f_m = f_{m2}$, $g_m = g_{m2}$, for lengthening. One can see that $V_{\max}$ plays the role of the maximum shortening velocity at which $P_V^{(short)} = 0$, and V_{m2} is a characteristic velocity separating slow and fast lengthening. Also, the limiting tension in the fastest steady lengthening is $P_{-\infty}^{(stret)} = 2P_0$.

.

3.3. CB domains

The force-velocity fitting analysis alone does not provide details on the CB attachment-detachment rates or the domains. Physically, these domains follow from the conditions of realization of thermodynamic stability described by a minimum of Gibbs energy (Hill et al., 1975). Nevertheless, the overall curve conditions of observation can be established here by the inequalities $\sigma_{m1}^{(\exp)} > 1 \geq \sigma_{m2}^{(\exp)}$, resulting from Eqs. (19) and (20), where the fitting parameter $\sigma_{m1}^{(\exp)} = \Phi(0.85)^{-1} = 1.22$ is found for muscle shortening and $\sigma_{m2}^{(\exp)}$, generally lying between 0.8 and 1.0, for lengthening.

Alternatively, the observation conditions of the predicted branches of the master curve can be reformulated in terms of the CB rigor state proportions $n_{01} < x_{m1}dx_{01}^{-1}(x_{01} + x_{m1})^{-1}$ and $n_{02} \geq x_{m2}dx_{02}^{-1}(x_{02} + x_{m2})^{-1}$, obtained with the help of Eq. (18). This finding can be improved when the CB geometrical constraints shown in Fig. 1 are taken into account. Indeed, since the tail of the myosin molecule is longer than heads, one should expect a

geometrical constraint $x_{m2} > x_{m1}$, providing $n_{02} > n_{01}$. Under the simplified requirements of periodicity ($x_{01} + x_{m1} = d$ and $x_{02} = x_{m2} = d$), the CB proportions underlying the observation of the master curve are specified in the insets in Figs. 2 and 3.

.

4. Discussion

Huxley's model of the establishment of mechanical equilibrium of myosin heads near actin-filament sites is based on the simplest kinetic equation determining a balance between unbound and bound actin-myosin states. In a muscle contracting at constant velocity V, these two states are described by the proportions $1 - n_V(x)$ and $n_V(x)$, satisfying the steady-state kinetic equation (2) at generally arbitrary rates $f(x)$ and $g(x)$. Such a property, following evidently from the solution $n_V(x)$ found for a general case in Eq. (9), implies that the kinetic equation accounts for the most general features of muscle relaxation, regardless of details underlying the attachment-detachment mechanism of myosin heads. Consequently, theoretical studies exploring an arbitrary choice of the functional form of the attachment-detachment rates, which involved increasing number of numerical parameters, guarantee good fit to phenomenological data, but do not shed light on the muscle intrinsic characteristics.

After work by Rayment et al. (1993) on the structural study of force generators in contracting muscles, the observations of catalytic domains of myosin being initially weakly attached to actin are commonly associated with the *weakly bound* CB states, and the following structural changes resulting in tight binding of actin-myosin linkages are associated with *strongly bound* CB states. Since the steady-state equation (2) is a late-time part of more general kinetic equation (1), the proportions $n_V(x)$ are also part of the non-steady solutions, as demonstrated by Lombardi and Piazzesi (1990) and recently by Walcott and Herzog (2008) employing Huxley's Eqs. (4) and (5). It seems therefore plausible to associate Huxley's short-domain proportion $n_V^{(loc)}(x)$ and large-domain proportion $n_V^{(deloc)}(x)$ with respectively weak and strong late-time CB states. In this study, the actin-myosin bound state is composed of the equilibrated and excited states distributed by Gaussian function dictated by the second law of thermodynamics.

Within the proposed framework of stochastic approach to the attachment-detachment events of myosin heads, a common requirement of normalization of the random proportion $n_V(x)$ specifies the heterogeneity of the CB distribution via the correlated intrinsic structural

(x_m, d), kinetic (f_m, g_m) and dynamic (V_m) muscle characteristics [see e.g. Eq. (14)], that decreases the number of free parameters. Moreover, the trend of weakly bound myosin heads to achieve maximum structural-domain entropy in the vicinity of actin-filament sites ($x \approx 0$) requires a correlation in signs between the head displacements (x) and velocities ($\dot{x}$). Consequently, the conceivable CB domains for both bound states schematically shown in Fig. 1 are eventually described by Heaviside functions in Eq. (15). A geometrical selection of the main components of the force resulting in the power stroke in a direction consistent with the vector of contraction velocity are also shown in Fig.1.

The explicit solution (9) to Huxley's kinetic equation for CB proportions $n_0(x)$ and $\Delta n_V(x)$, distributing respectively strongly and weakly bound states over the actin filament cells, results in the velocity-independent (isometric) force F_0 and contractive force ΔF_V, components of the CB force output F_V (16). In Fig. 2, famous Huxley's comparative analysis with Hill's data on muscle concentric tension (Huxley, 1957, p. 287) is revisited. The high-velocity wing of the tension curve above $V/V_{\max} = 0.5$ controlled mostly by weak CB states is well fitted by both non-Gaussian (5) and Gaussian (15) proportions. It is not the case of the low velocity region $0.2 < V/V_{\max} < 0.5$, where a discrepancy between Huxley's curve (8) and the data indicate a disadvantage of the short-domain ($x < h < d$) weak CBs exerting negative force ΔF_V and eventually reducing the total produced tension. In contrast to the postulated retarded detachment ($g_1 < f_1$) discussed in Eqs. (4) and (7), the Gaussian strong and weak CBs require faster detachment than attachment ($g_{m1} > f_{m1}$) in muscle shortening, as derived from Hill's data and shown in the inset in Fig. 2. The regular deviation of Gaussian CBs from the data at very low velocities is associated with a simplified modeling of the channel of relaxation of weak states to strong states. Indeed, the fit analyses can be improved when the proportion of a new weak-to-strong transient Gaussian CB spreads its domain symmetrically within the range $-\delta \leq x \leq \delta$, extending the weak CB state in the vicinity of $x \approx 0$, as shown by the dotted line in the inset in Fig. 2 for the case $V/V_{\max} = 0.1$.

In Fig. 3, the upper branch of the force-velocity curve (18) drawn at a single adjustable parameter ($V_{m2} = -288\ nm/s$) fits well the empirical data on CB force in muscle stretching. Similar to shortening, the fitting analysis could be improved at low stretch velocities when a transient bound state is additionally introduced, as independently proposed by Mehta and Herzog (2008, Fig. 3). These authors also raised the central question on the existence of

Huxley's proportions favoring myosin head attachment events at large distances with an increase in contraction velocity. One therefore infers that although non-Gaussian large-domain CBs (5) numerically fit the empirical data (Fig. 2), they do favor neither thermodynamic equilibrium in the overlapped zone nor high cycle efficiency (Hill et al., 1975).

The microscopic structures of the short-domain bound states are provided above via observation conditions of the generic curve (18) equally applied to the reduced tension in a single CB, sarcomere, fiber, or muscle as a whole during its steady shortening or lengthening. It is also demonstrated (inset in Fig. 3) how the two-state muscle cycle *duty ratio* β derived from real experiments can be helpful in a characterization of the Gaussian CB *rate ratio* $\alpha = f_m/g_m$ $[= (1-\beta)/\beta]$ and strong bound state proportion n_0 $(= 1-\beta)$. To summarize a comparative analysis of structural and kinetic characteristics of CBs, one can see that *steady* muscle eccentric and concentric contractions are well distinguished via the attachment-detachment rate rations, with $\alpha_{stret} > 1 > \alpha_{short}$, the strongly-bound occupation numbers, with $n_0^{(stret)} > n_0^{(short)}$, supported by the directly observable cycle duty ratios $\beta_{stret} < \beta_{short}$ (Mehta and Herzog, 2008). Within this context, the working hypothesis by Mehta and Herzog (2008) "that a stretched cross-bridge might remain attached longer than a cross-bridge that had been shortened while attached" combined with the main finding by Lombardi and Piazzesi (1990) that "reattachment (in steady lengthening is)... faster than attachment in the isometric condition or during shortening ... in the same domain of x" results in the predictions $\alpha_{stret} > 1$, $n_0^{(stret)} > 1/2$, and $\beta_{stret} < 1/2$, which are generally consistent with the CB parameters derived in the insets in Figs. 2 and 3.

To conclude, the provided statistical thermodynamic analysis of the attachment-detachment CB process, modifying Huxley's mechanical sliding filament model, can also be figured out as an two-headed steady walking of synchronous myosin molecules over periodical sites of actin filaments with multiple 36-nm steps, as directly observed by Sakamoto et al. (2008). The fluctuating steps are statistically scattered by the normal distribution, having the zero mean and variance linear with muscle contraction velocity. The proposed steady contraction dynamics is universally observable through the two branches of the force-velocity curve generic for steady shortening and lengthening of a muscle as a whole or its counterparts. The microscopic structural muscle characteristics appear to be strongly correlated to kinetic and dynamic characteristics distinguished by the force output directions generated in distinct muscle regimes. At a macroscopic level, similar kind of correlations

driven by maximum generated force were revealed via the primary muscle functions well distinguished though the muscle structure adapted to efficient eccentric, isometric, or concentric contractions (Kokshenev, 2008).

.

Acknowledgements

.

The author thanks Scott Medler for helpful comments. The financial support by CNPq is also acknowledged.

.

References

Cole, G. K., Bogert, A. J., Herzog W., Gerritsen, K. G. M., 1996. Modelling of force production in skeletal muscle undergoing stretch. Journal of Biomechanics, 29, 1091-1104.

Craig, R., Woodhead, J. L., 2006. Structure and function of myosin filaments. Current Opinion in Structural Biology, 16, 204–212.

Eisenberg, E., Hill, T.L., Chen, Y.D., 1980. Cross-bridge model of muscle contraction. Quantitative analysis, Biophysical Journal, 29, 195-227.

Harry, J. D., Ward, A. W., Heglund, N.C., Morgan, D. L., McMahon, T. A., 1990. Cross-bridge cycling theories cannot explain high-velocity lengthening behavior in frog muscle, Biophysical Journal, 57, 201-208.

Hill, A. V., 1938. The heat of shortening and the dynamic constants of muscle. Proceedings of Royal Society of London, 126, 136-195.

Hill, T.L., Eisenberg, E., Chen, Y., Podolsky, R. J., 1975. Some self-consistent two-state sliding filament models of muscle contraction. Biophysical Journal, 15, 335-372.

Huxley, A. F., 1957. Muscle structure and theories of contraction. Progress in Biophys. Biophys. Chemistry, 7, 255-318.

Huxley, H. E., Hanson, J., 1954. Changes in the cross-striations of muscle during contraction and stretch and their structural interpretation. Nature, 173, 973-976.

Huxley, A. F., Niedergerke, R., 1954. Interefrenec microscopy of living muscle fibers. Nature 173, 971-973.

Huxley, A. F., Simmons, R. M., 1971. Proposed mechanism of force generation in striated muscle. Nature 233, 533-538.

Huxley, A.F., 1998. Biological motors: Energy storage in myosin molsecules. Current

Biology, 8, R485-R488.

Kokshenev, V. B., 2008. A force-similarity model of the activated muscle is able to predict primary locomotor functions. Journal of Biomechanics, 41, 912–915.

Landau L. D., Lifshitz, E. M., 1989. Statistical Physics, Pergamon Press, London.

Lombardi, V., Piazzesi, G., 1990. The contractile response during steady lengthening of stimulated frog muscle fibres. The Journal of Physiology 431, 141-171.

Ma, S., Zahalak, G. I., 1991. A distribution-moment model of energetics in skeletal muscle. Journal of Biomechanics, 24, 21-35.

Mehta, A., Herzog, W., 2008. Cross-bridge induced force enhancement? Journal of Biomechanics, 41, 1611-1615.

Rayment, I., Holden, H. M., Whittaker, M., Yohn, C.B., Lorenz, M., Holmes, K.C., Milligan, R.A., 1993. Structure of the actin-myosin complex and its implications for muscle contraction. Science, 261, 58-65.

Sakamoto, T., Webb, M. R., Forgac, E., Howard, D. White, H. D., Seller, J.R. 2008. Direct observation of the mechanochemical coupling in myosin Va during processive movement. Nature 455, 128-132.

Walcott, S., Herzog W., Modeling residual force enhancement with generic cross-bridge models, 2008. Mathematical Biosciences, 216, 172–186.

Wu, J.Z., Herzog W., Cole G. K., 1997. Modeling dynamic contraction of muscle using the cross-bridge theory, Mathematical Biosciences, 139, 69-78.

Zahalak, G. I., 1981. A distribution-moment approximation for kinetic theories of muscular contraction. Mathematical Biosciences, 55, 89-114.

Figure Legends

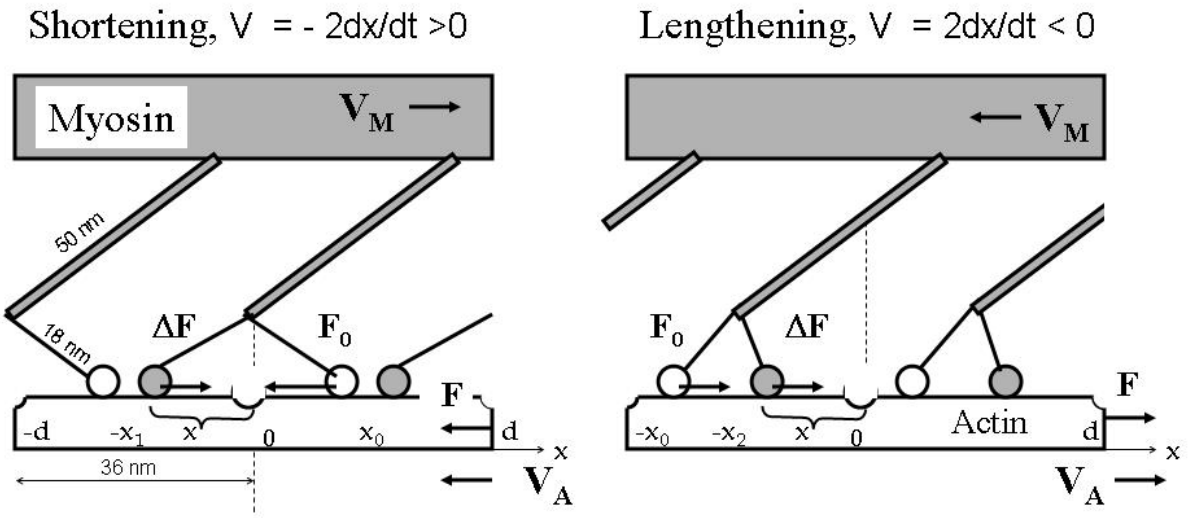

Fig. 1

Figure 1. Mechanical scheme of the force generation by combining myosin heads with periodic actin filament. Each of the two heads of the effective CB may be attached to actin filament either in equilibrated ground state (shown by the open circle) with the uniform probability n_0, within the domains $x \leq \pm x_0$, or in the non-equilibrium, excited state (closed circle) with the probability $\Delta n_V(x)$, within the domains $x \leq -x_1, -x_2$. The *arrows* indicate the directions of the sliding velocity of the actin filament V_A and the myosin filament V_M. During concentric muscle contraction with a *positive* velocity V, the velocity-independent portion of the generated force F_0 is also positive, whereas the ATP hydrolysis results in the negative portion of the contractive force ΔF_V . During eccentric contractions commonly associated with the *negative* direction of velocity V, both the forces are also negative.

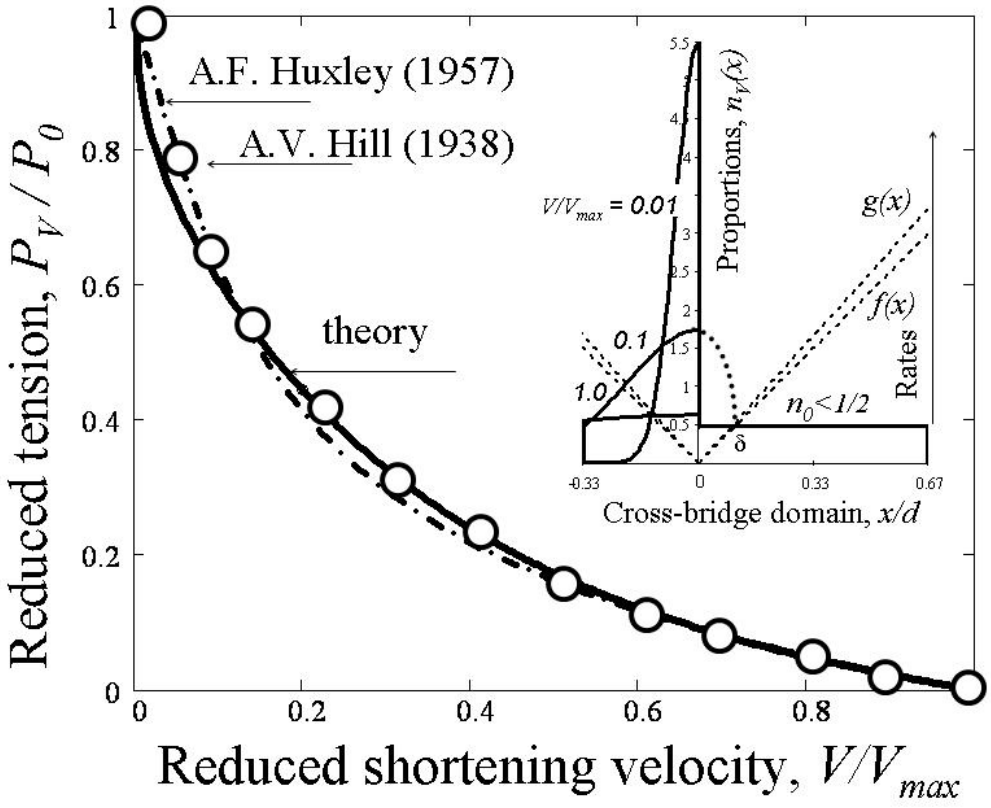

Fig. 2

Figure 2. Analysis of the theoretically predicted tension-velocity curve using available data on the reduced tension during steady muscle shortening. The *points* and *dashed-point curve* are the famous data by Hill (1938) for isolated frog muscles modeled by Huxley (1957), drawn respectively by the phenomenological equation $P^{(\mathrm{exp})}/P_0 = a(1-V/V_{\max})/(a+V/V_{\max})$, with $a = 0.25$ and Eq. (8), fitted by Huxley's parameters listed above. The *solid line* is Eq. (19) taken at $\lambda = 0.85$. *Inset:* The attachment-detachment rates and CB proportions predicted in Eq. (15) within the CB domains at distinct shortening velocities reduced to the maximum velocity. The CB structure discussed in the Results is exemplified by the model parameters $x_{01}^{(\mathrm{mod})} = 2d/3$ and $x_{m1}^{(\mathrm{mod})} = -d/3$, as well as by $n_{01}^{(\mathrm{mod})} = 0.47$, providing the *rate ratio* $\alpha_1 = f_{m1}/g_{m1} = 0.88$. The *dotted line* shows a proportion for the modeled transient CB state schematically drawn for $V/V_{\max} = 0.1$.

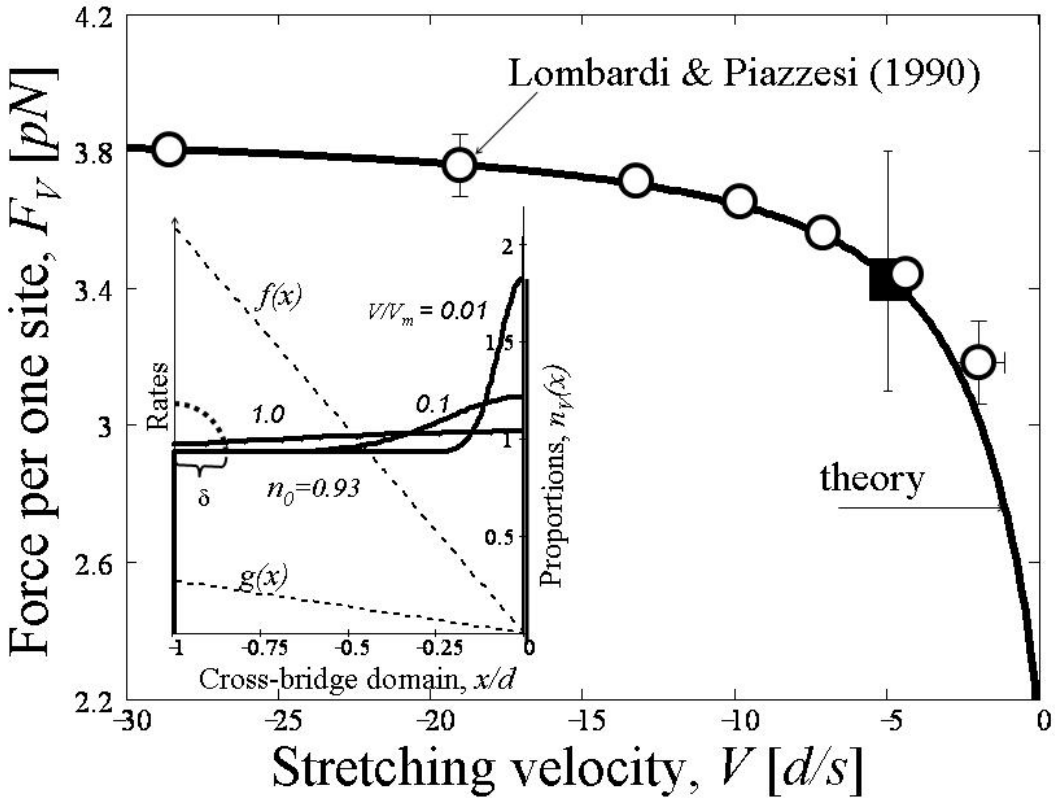

Fig. 3

Figure 3. Steady force induced by one cross-bridge versus the stretching velocity. The *open circles* are the mean datapoints of the forces (re-scaled by $|F_0| = 1.95\,pN$) measured by Lombardi and Piazzesi (1990, Fig. 7) in frog muscle fibers at stretch velocities lying between 75 and 1030 nm/s and scaled here by $d = 36\ nm$. The *closed square* indicates the force per one CB reported by Mehta and Herzog (2008) for unspecified velocities. The theoretical curve is drawn based on Eq. (20) with $V_{m2}^{(\mathrm{mod})} = -8\ d/s$. *Inset:* The attachment-detachment rates within the CB domains and CB proportions predicted in Eq. (15) at three distinct velocities reduced to the found $V_{m2}^{(\mathrm{mod})}$. They are exemplified by model parameters $x_{02}^{(\mathrm{mod})} = x_{m2}^{(\mathrm{mod})} = -d$, consistent with the observation conditions discussed in the Results, as well as by $n_{02}^{(\mathrm{exp})} = 1 - \beta_2^{(\mathrm{exp})} = 0.93$, where the stretch *cycle duty ratio* $\beta_2^{(\mathrm{exp})} = 7.35\%$ (the time of attachment f_m^{-1} related to total CB cycling time $f_m^{-1} + g_m^{-1}$, i.e., $\beta = 1 - n_0$) studied by Mehta and Herzog (2008) is employed. Moreover, the relation $|V_{m2}^{(\mathrm{mod})}| = f_{m2}^{(\mathrm{exp})} x_{m2}^{(\mathrm{mod})} / [1 - \beta_2^{(\mathrm{exp})}]$ derived from Eq. (20) provides a crude model estimate for the CB domain $x_{m2}^{(\mathrm{mod})} \approx 1.2\ d$, if their characteristic attachment time $[f_2^{(\mathrm{exp})}]^{-1} = 0.167\ s$ is also employed. The rates (shown

by *dashed lines*) are determined by the ratio $f_{m2}^{(\mathrm{exp})}/g_{m2}^{(\mathrm{mod})} = 13$, corresponding to the model estimate $[g_{m2}^{(\mathrm{mod})}]^{-1} = 2.2\ s$. The *dotted line* shows a proportion for the assumed transient CB state schematically drawn for $V/V_{m2}^{(\mathrm{mod})} = 0.1$.